Tuning the coverage of self-assembled monolayer by introducing bulky substituents onto rigid adamantane tripod

Toshikazu Kitagawa,*[a] Shima Nakanishi,[a] Aya Mizuno,[a] Yohei Niwa,[a] Hiroki Tabata,[a] Katsuyuki Hirai,[b] and Takao Okazaki*[a]

[a] *Department of Chemistry for Materials, Graduate School of Engineering, Mie University, Tsu, Mie 514-8507, Japan*
[b] *Organization for the Promotion of Regional Innovation, Mie University, Tsu, Mie 514-8507, Japan*
Email: kitagawa@chem.mie-u.ac.jp

*Dedicated to Professor Kenneth K. Laali on the occasion of his 65th birthday*

Abstract

An area-demanding tripodal trithiol containing six peripheral methyl groups was synthesized, and its self-assembled monolayer (SAM) was formed onto a Au(111) surface, which was electrochemically characterized. The SAM showed a significant lowering of the surface coverage due to the bulkiness of the methyl groups, as demonstrated by the charge of reductive elimination. The experimentally determined surface density was aptly reproduced by density functional theory (DFT) calculations under periodic boundary conditions.
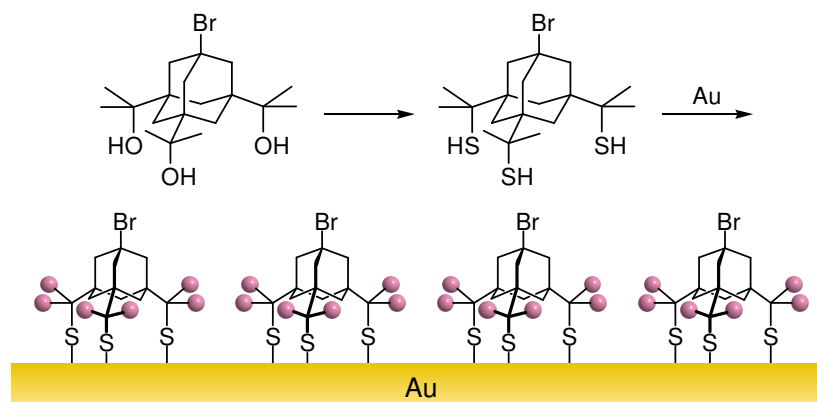
Keywords: Molecular tripod, self-assembled monolayer, adamantane, thiol, gold substrate

Introduction

Thiols are readily chemisorbed on gold surface and form tight Au–S bond. Densely packed monolayers can be spontaneously constructed by simply immersing metallic gold into a thiol solution.[1–3] Self-assembled monolayers (SAMs) prepared in this manner have attracted a great deal of attention for their utility in a variety of functional molecular assemblies that include molecular sensors,[4,5] molecular machines,[6,7] and molecular electronic devices.[8,9] We previously reported that tripod-shaped trithiol **1**, composed of a rigid adamantane core and three CH_2SH legs, forms a SAM on Au(111) with a highly ordered arrangement by three-point adsorption (Figure 1).[10] Based on the results of scanning tunneling microscopy (STM) measurements, the SAM showed hexagonal (3 × 3)R60° packing with a closest molecular distance of 8.7 Å, which is a significantly larger distance than that normally observed for the SAMs of linear alkane thiols (5.0 Å). Such a large distance allows SAMs of functional molecular units, connected at the top of the tripod, to be adsorbed without strong molecular interaction, which is sometimes unfavorable for the construction of functional SAMs.[11,12]
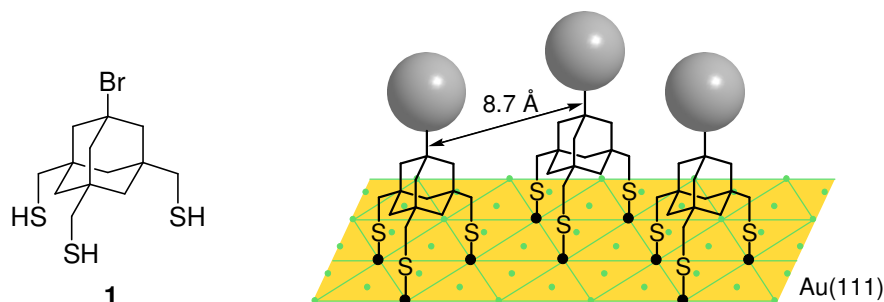

Figure 1. Tripodal trithiol with an adamantane core **1** and its SAM on a Au(111) surface.[10] The gray spheres represent functional molecular unit.

    In order to connect larger functional molecules, a more sterically demanding tripod is required to avoid molecular interactions within a SAM. In this paper, we report the synthesis of an adamantane tripod with three CMe_2SH groups **2** (Figure 2). Due to the bulkiness of the protruding methyl groups, this molecule is expected to occupy a significantly larger surface area when adsorbed onto Au. The preparation of a SAM of **2** on Au(111) substrate is described, along with experimental and theoretical evaluations of the extended molecular distance.
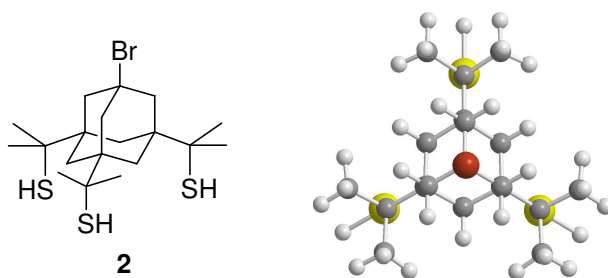

Figure 2. Sterically demanding hexamethylated molecular tripod **2**.

Results and Discussion
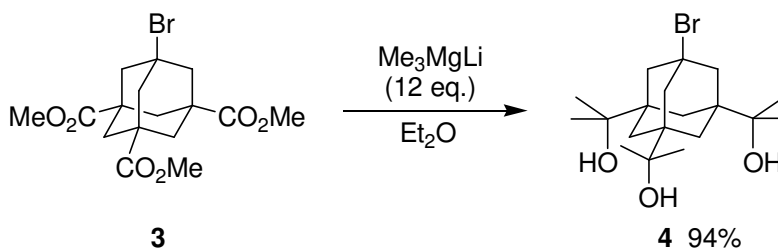
Synthesis of a trithiol

A common strategy for the synthesis of aliphatic thiols involves the conversion of the corresponding alcohols. Primary alcohols can be converted to thiol derivatives by converting the hydroxy group to a good leaving ester group, followed by a subsequent S_N2-type substitution using a sulfur nucleophile.[10–12] The conversion into **2**, with three tertiary thiol groups, however, requires substitution via a carbocationic intermediate under acidic conditions. In the present study, the starting alcohol is a hexamethyl triol **4**. A good precursor of this triol is triester **3**, which we synthesized earlier as a precursor of **1**.[10]

The synthesis of tertiary triol **4** via an exhaustive methylation of triester **3** requires multiple nucleophilic additions to the methoxycarbonyl groups bound to a bulky adamantyl group. The treatment of **3** with a large excess (12 eq.) of MeMgI at 0 °C, however, gave **4** in only 20% yield along with a large amount of incompletely methylated products **5** and **6** (Scheme 1). Complete methylation was achieved at 50 °C, but a concomitant loss of bromo group occurred at this temperature to give a considerable amount of unknown compounds.

3:4:5:6 = 11:20:49:20 (by NMR)
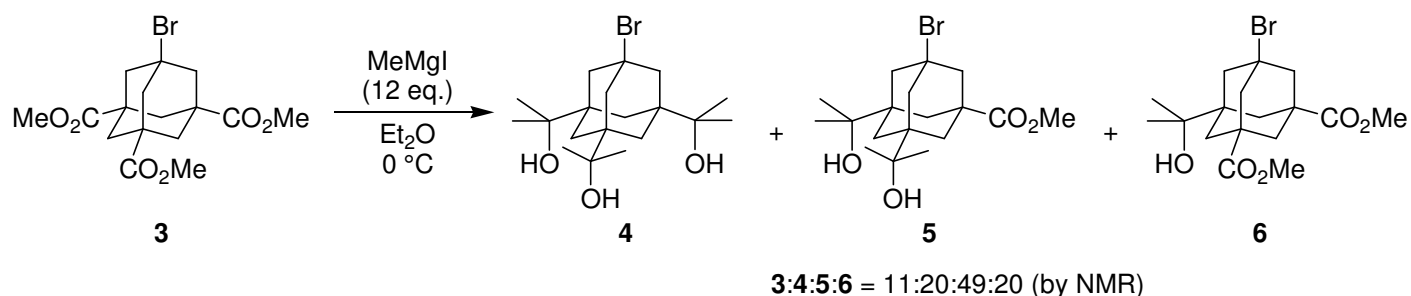
**Scheme 1.** Reaction of triester **3** with methylmagnesium iodide.

Ishihara[13] has reported that the nucleophilicity of a Grignard reagent is greatly strengthened by the formation of R_3MgLi ate complexes with two equivalents of organolithium, which gives "Grignard" products in high yields from ketones that are amenable to reduction or to aldol reaction. The methylation of triester **3** using twice the stoichiometric amount of Me_3MgLi proceeded very cleanly, giving essentially pure triol **4** almost quantitatively (Scheme 2).

Scheme 2. Synthesis of trithiol **4** using a magnesium ate complex.

To establish a satisfactory method for the synthesis of trithiol **2**, several reactions were examined using tertiary monoalcohol **7** as a model compound. An S_N1-type substitution of trifluoroacetate **8** in polar solvents using crown ether-activated potassium thioacetate as a nucleophile gave a complex mixture [Scheme 3, (a)]. Treatment of **8** with NaSH-treated Amberlite, which is reportedly pertinent for some tertiary thiols,[14] was not

effective, resulting also in unidentified products [Scheme 3, (b)]. These results could be attributed either to facile elimination or to the skeletal rearrangement of intermediate carbocation.
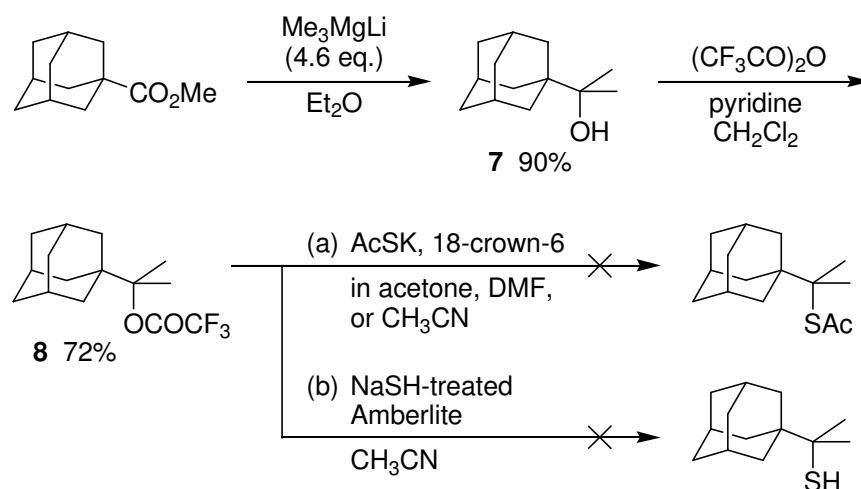
Scheme 3. Attempts at the conversion of alcohol **7** to trifluoroacetate **8** and to thiol derivatives.

As an alternative method, Schreiner has demonstrated that tertiary alcohols can be converted to the corresponding thiols by treatment with thiourea in the presence of hydrobromic and acetic acids and subsequent alkaline hydrolysis.[15] The thiolation of monoalcohol **7** gave thiol **9** along with a byproduct alkene **10** (Scheme 4). The selectivity was modified by lowering the temperature of the first step (Table 1), giving an optimal yield of 97% at 25 °C with no detectable formation of the alkene (entry 6).
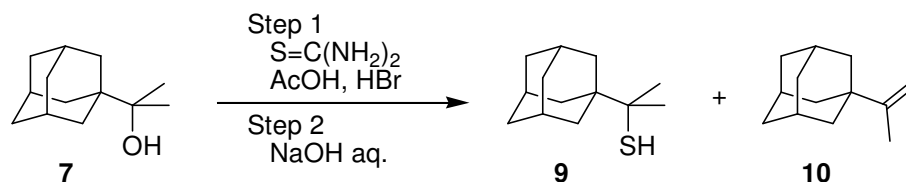
Scheme 4. Thiolation of monoalcohol **7** with thiourea treatment.

Table 1. Optimization of the thiolation of **7**

entry	temp (°C)[a]	time (h)[a]	molar ratio[b]		
			9	**10**	**7**
1	130	3	87.3	1.7	11.0
2	95	6	90.7	1.1	8.2
3	80	6	92.8	0.8	6.4
4	65	6	94.1	0.4	5.5
5	50	6	95.6	0.2	4.2
6	25	6	97.0[c]	0.0	3.0

[a] Temperature and time in step 1. [b] From ^{1}H NMR peak integration. [c] Pure thiol **9** was isolated in 90% yield after separation.

Following the successful thiolation of model alcohol **7**, we applied this method to the synthesis of trithiol **2** (Table 2). Unlike the synthesis of monothiol **9**, however, no significant reaction was observed at 25 °C (entry 1). At higher temperatures the ^{1}H NMR spectra of the product mixture showed methyl protons of the -CMe$_2$SH group at δ 1.42. Along with this signal there were also signals of the methyl group of unchanged -CMe$_2$OH group (δ 1.21) and the olefinic protons of the -CMe=CH$_2$ group (δ 4.77), suggesting the formation of a multi-component mixture shown in Scheme 5, which consisted of partially thiolated products **11** and **12** and of elimination products such as **13** and **14**. The abundance ratios of these groups were calculated from NMR integrations for reactions under different conditions and are summarized in Table 2.
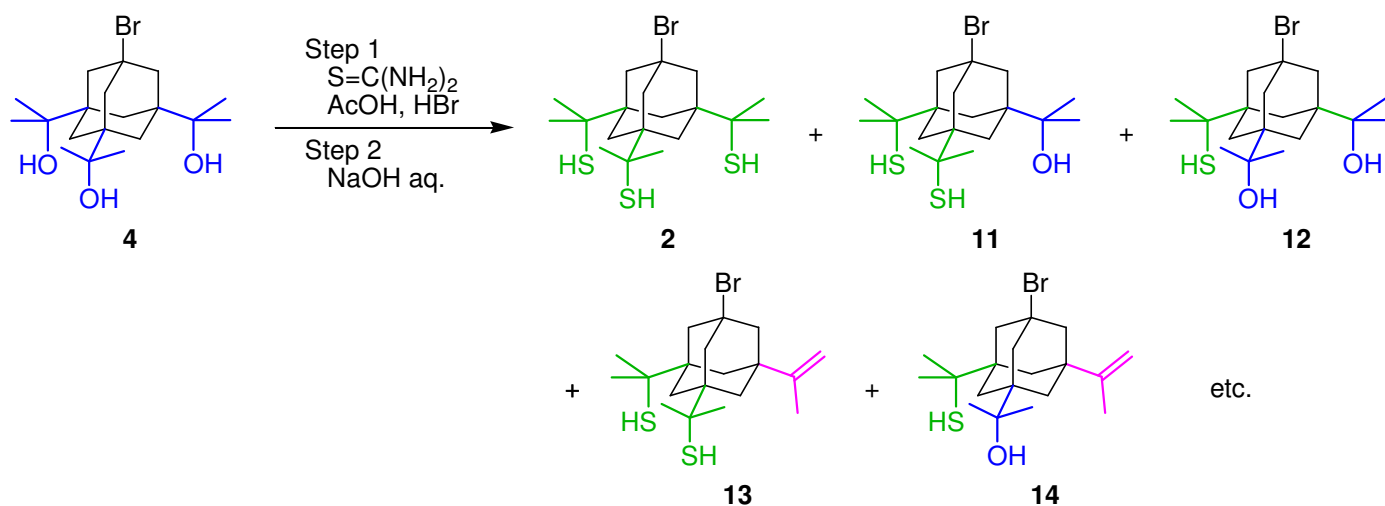
Scheme 5. Thiolation of triol **4** by thiourea treatment.

Table 2. Optimizing the trithiolation of **4**

| entry	step 1			step 2		relative ratio[a]		
	temp (°C)	time (h)	thiourea (eq.)[b]	temp (°C)	time (h)	-CMe$_2$SH	-CMe$_2$OH	-CMe=CH$_2$
1	25	6	150	rt	15	0	94	6
2	50	6	150	rt	15	51	43	6
3	70	10	150	rt	15	70	23	7
4	70	24	150	rt	15	70	22	8
5	90	10	150	rt	15	66	22	12
6	70	14	150	0	15	70	22	8
7	70	14	150	0	3	71	20	9
8	70	14	450	0	3	77	18	5
9[c]	70	14	450	0	3	94	4	2

[a] From ^{1}H NMR peak integration. [b] Molar ratio thiourea/**4**. [c] The product mixture from entry 8 was used as the starting material. The final product ratio was **2:11:13** = 82:12:6. Pure **2** was isolated in 21% yield after separation.

The conversion from OH to SH group increased when the temperature of step 1 was raised (entries 2–5), but a prolonged reaction time at 70 °C did not change the ratio, because the initial acid-catalyzed substitution

by thiourea was not completed due to the equilibrium shown in Scheme 6. Since elimination became significant at 90 °C, heating at 70 °C for 10 h (entry 3) was considered optimal.

The selectivity of thiol and alkene formation is determined in step 2 and depends on the position of the attack from the hydroxide ion (Scheme 6, A and B). Although the temperature and the time for step 2 were reduced in entries 6 and 7, no desired modification of the selectivity was achieved.

Next, the equilibrium in step 1 was shifted to the right by the use of a large excess (450 eq.) of thiourea (entry 8), but a complete conversion of OH to SH remained a difficult task, and 18% of -CMe_2OH remained unchanged. To further convert this to a -CMe_2SH group, the product mixture of entry 8 was retreated by the same procedure to give a crude trithiol **2** that contained 12% of **11** and 6% of **13** (entry 9). After removing alcohol **11** by flash chromatography, **2** and **13** could be separated by careful gel permeation chromatography to afford pure **2** in 21% yield.
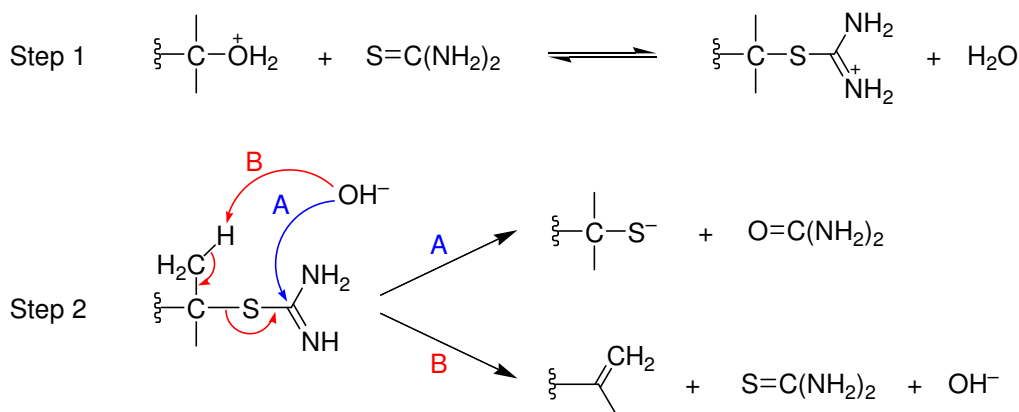
Scheme 6. Two steps of the thiolation of alcohol by thiourea.

Formation of the SAM on Au(111) and XPS characterization

The SAMs of tripodal trithiol **2** were prepared by immersing a gold substrate, Au(111), with a thickness of 200 nm on mica, into 0.1 mM solutions in dichloromethane at an ambient temperature for 15 h or longer. The SAM-modified substrate was washed thoroughly with dichloromethane and air-dried.

The state of the adsorbed thiolate molecules was examined by X-ray photoelectron spectroscopy (XPS) measurement. A sulfur atom bound to gold was reported to show $2p_{3/2}$ and $2p_{1/2}$ signals at 161.9–162.0 and 163.2 eV, respectively, with a 2:1 intensity ratio.[16,17] The SAM of **2** exhibited a signal at 162.0 eV, corresponding to the chemisorbed sulfur atoms (Figure 3). Unbound free SH group, which is expected to appear at 163.5 ($2p_{3/2}$) and 164.8 ($2p_{1/2}$) eV,[18] was not detected, consistent with three-point adsorption.
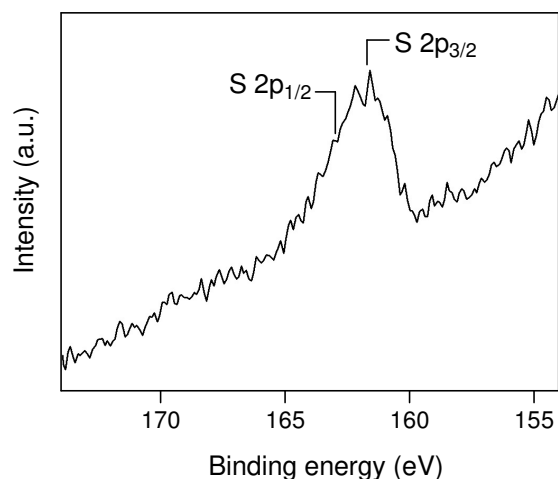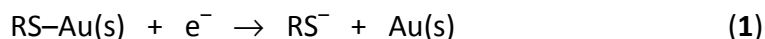
Figure 3. X-ray photoelectron spectrum of the SAM of **2** on Au(111), prepared from a CH_2Cl_2 solution.

Electrochemical reductive desorption of thiolate ion

Figure 4 shows a cyclic voltammogram of the SAM of **2** recorded in aqueous KOH. A negative current peak due to the desorption of thiolate ion (Equation 1)[19,20] was observed at −0.930 V vs Ag/AgCl.

$$RS–Au(s) \ + \ e^− \ \rightarrow \ RS^− \ + \ Au(s) \qquad\qquad (1)$$

The observed peak potential and the charge of the reductive desorption of tripod **2** are summarized in Table 3, together with the values for *n*-dodecanethiol and our previous trithiol **1**. The SAM of **2** underwent desorption at a less negative potential than that of **1**, which may indicate the weakness of the sulfur-gold bonding in the former SAM (*vide infra*).

In our previous study, the SAM of **1** showed the same reductive charge (100 $\mu C/cm^2$)[21] as that of *n*-dodecanethiol SAM, because in both SAMs the sulfur atoms are packed in essentially the same hexagonal pattern shown in Figure 1.[10] Chemisorption of sulfur atoms with the same density is not possible for **2** since
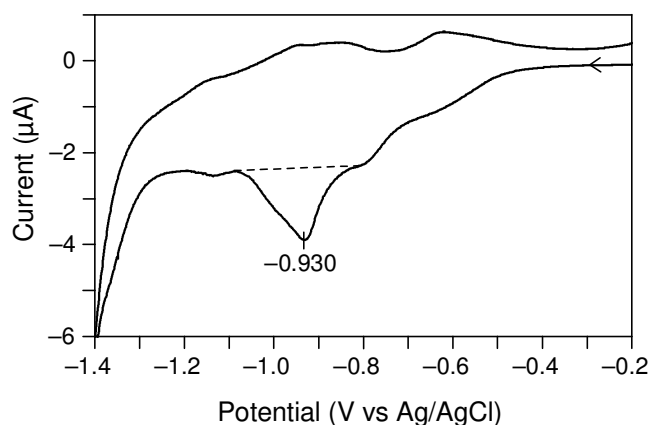

Figure 4. Cyclic voltammogram for the reductive desorption of the SAM of **2** on a Au(111) working electrode in 0.5 M KOH. Scan rate, 20 mV/s. Geometric area of the working electrode, 0.152 cm^2. The charge for reductive desorption was calculated from the area below the dotted line.

the molecule occupies a larger surface area. A reductive charge of 65±7 µC/cm^2, was observed for this SAM, indicating that the molecular distance is $(100/65)^{1/2}$ = 1.24 times greater than the SAM of **1**. This corresponds to an elongation of average distance to 10.8 Å, if the tripod molecules are assumed to be hexagonally arranged.

Table 3. Peak potential and charge for the electrochemical reductive desorption of SAMs derived from thiols on Au(111)[a]

thiol	peak potential (V vs Ag/AgCl)	reductive charge (µC/cm^2)[b,c]	intermolecular distance (Å)[c]	ref.
n-C$_{12}$H$_{25}$SH	−1.084	100	5.0	10
1	−1.088	100	8.7	10
2	−0.930	65[d]	10.8	this work

[a] Measured by cyclic voltammetry in 0.5 M aqueous KOH. Scan rate, 20 mV/s. [b] Calculated by integrating the cathodic wave. [c] Uncertainty due to sample-to-sample variations, ±10%. [d] Average of four runs.

Theoretical prediction of molecular packing in the monolayer on gold

The adsorption energy (E_{ads}) of adamantane tripod molecules Ad(CX$_2$S)$_3$ (X = H, Me) on a gold surface is expressed as follows.

$$E_{ads} = E[Ad(CX_2S)_3/Au\ layer] - E[Ad(CX_2S)_3] - E(Au\ layer) \tag{2}$$

In this equation, $E[Ad(CX_2S)_3/Au\ layer]$, $E[Ad(CX_2S)_3]$, and $E(Au\ layer)$ are the energies of Au layer with adsorbed Ad(CX$_2$S)$_3$, free Ad(CX$_2$S)$_3$, and Au layer, respectively.[22]

   Initial calculations of tripod-adsorbed surface structures were performed for Ad(CX$_2$S)$_3$ molecules (X = H or Me) adsorbed onto a Au monolayer composed of 19, 27, or 37 Au atoms as models of the Au(111) surface (Figure 5). Several energy minima were obtained (see Tables S1 and S2 in supporting information), among which **X1** and **X2** were found to be the most stable geometries for Ad(CH$_2$S)$_3$/Au layer and Ad(CMe$_2$S)$_3$/Au layer, respectively (Figure 6).
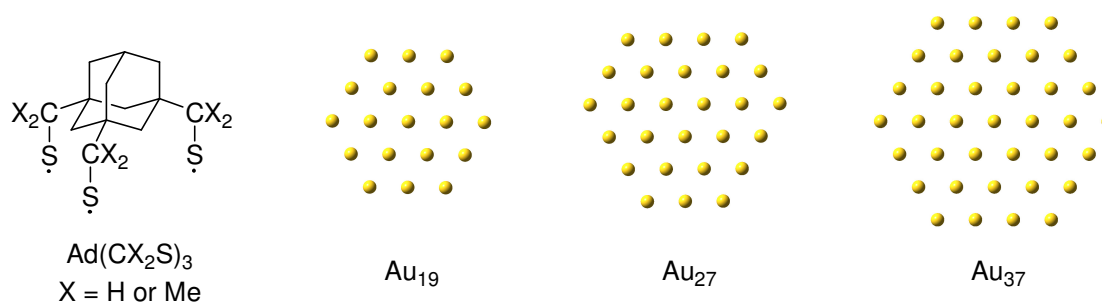
Figure 5. Structures of Ad(CX$_2$S)$_3$ and finite Au layers.

X1
Ad(CH₂S)₃ on Au₂₇
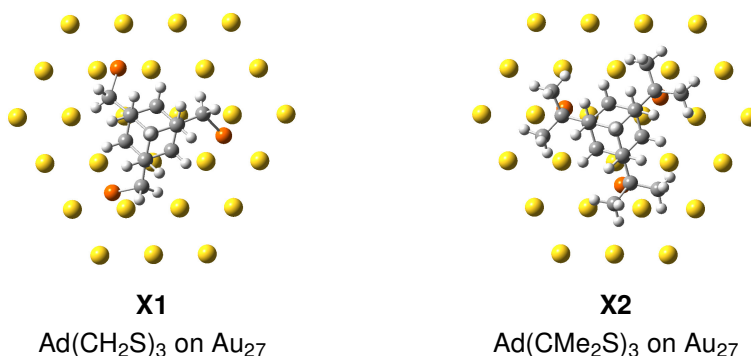
X2
Ad(CMe₂S)₃ on Au₂₇

Figure 6. Structures of Ad(CH₂S)₃ and Ad(CMe₂S)₃ on the Au₂₇ monolayer optimized by the DFT method.

In the next step, single-point energy calculations for the infinite SAM on Au(111) were conducted under two-dimensional periodic boundary conditions (PBC) using the geometries **X1** and **X2** (Table 4). Among eight possible orientations for the SAM of Ad(CH₂S)₃ (see Table S4 in Supporting Information for complete results), the (3 × 3)R60° lattice showed the most negative E_{ads} (–4.28 kcal/mol per Au atom). The nearest molecular distance was 8.64 Å, and the shortest intermolecular distances of H–H and S–S were 2.67 Å and 3.99 Å, respectively, which are longer than the van der Waals diameters of H and S atoms.[23] These results show that the (3 × 3)R60° orientation can provide a stable SAM from Ad(CH₂S)₃, which is consistent with the experimental observation of this arrangement for the SAM of molecule **1**.[10]

Table 4. Adsorption energy E_{ads} by PBC calculations for the SAMs of Ad(CH₂S)₃ and Ad(CMe₂S)₃ on Au(111)[a]

(i)   (ii)   (iii)
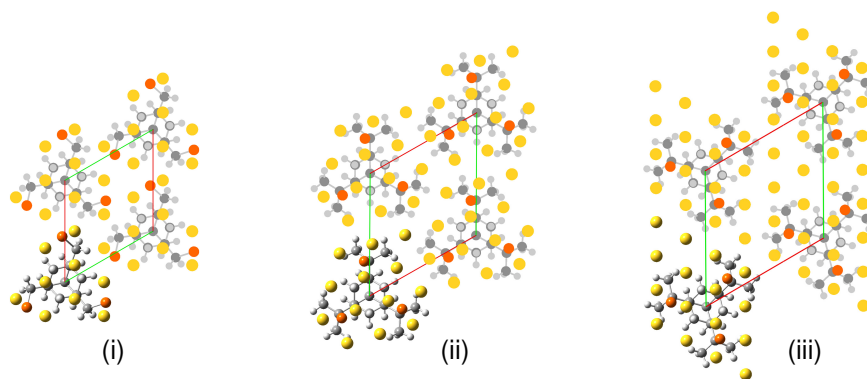
adsorbed molecule	unit cell[b]	structure of SAM	nearest molecular distance (Å)	number of Au atoms per unit cell	E_{ads} (kcal/mol)[c] per unit cell	per Au atom
Ad(CH₂S)₃	(3 × 3)R60°	(i)	8.64	9	–38.5	–4.28
Ad(CMe₂S)₃	($\sqrt{13} \times \sqrt{13}$)R46.1°	(ii)	10.38	13	–26.5	–2.04
	(4 × 4)R60°	(iii)	11.52	16	–25.6	–1.60

[a] UBLYP/3-21G for C, H, and S atoms and LanL2MB for Au atom. The Au-Au distance was fixed at 2.88 Å during structural optimization. [b] Wood's notation.[24,25] [c] $E_{ads} = E[Ad(CX_2S)_3/Au\ layer] - E[Ad(CX_2S)_3] - E(Au\ layer)$ (X = H or Me). E(Au layer) and $E[Ad(CX_2S)_3]$ were also calculated and are given in Tables S6 and S7, respectively.

For the hexamethylated molecule Ad(CMe$_2$S)$_3$, the (3 × 3)R60° lattice is impossible due to severe repulsion between adjacent molecules. On the other hand, (4 × 4)R60° showed a negative E_{ads} of −1.60 kcal/mol (per Au atom), and the value for ($\sqrt{13} \times \sqrt{13}$)R46.1°, −2.04 kcal/mol was lowest. The nearest molecular distances in these structures were 11.52 and 10.38 Å, respectively suggesting that the molecular packing of the SAM of trithiol **2** would fall within this range. This agrees well with the experimental value of 10.8 Å, from cyclic voltammetry. In addition, the calculated adsorption energies per unit cell suggest that the Au–S bond is weaker in the Ad(CMe$_2$S)$_3$ system. It is likely that the S atoms in this molecule are unable to take the most preferred positions on the Au(111) surface due to the steric effect of the methyl groups. This explains the observed less-negative peak potential of reductive desorption.

Conclusions

The synthesis of an area-demanding tripodal trithiol containing peripheral methyl groups **2** was achieved via exhaustive methylation of starting triester **3** using a magnesium ate complex to form triol **4** with subsequent thiourea-mediated thiolation. A SAM was prepared from this trithiol and was characterized by XPS and cyclic voltammetry. The observed charge for the reductive desorption and theoretical estimation of molecular packing by the PBC-DFT method indicated that **2** is distributed on SAM with a nearest molecular distance of ca. 10.8 Å. This length is 24% greater than we previously reported (8.7 Å) for the SAM of non-methylated tripod molecule **1**. The present results will allow the preparation of the monolayers of large functional molecular units without undesirable lateral interactions between neighboring molecular units.

Experimental Section

General. Anhydrous solvents used for synthesis were prepared by standard methods. Other reagents were used as received, unless otherwise noted. NMR spectra were obtained using either a JEOL JNM-A500 (^{1}H, 500 MHz; ^{13}C, 125 MHz) or a JEOL JNM-AL300 (^{1}H, 300 MHz; ^{13}C, 75.5 MHz) instrument. High-resolution mass spectra were obtained using a JEOL JMS-600H spectrometer. The IR spectra were recorded on a JASCO FT/IR-4200 spectrophotometer with an attenuated total reflection (ATR) mode. Preparative gel permeation chromatography was performed in a recycle mode using a Shodex H-2001 column (20 mm × 50 cm).

2-(1-Adamantyl)-2-propanol (7).[26] A solution of CH$_3$MgI in ether (9 mL) was prepared from 0.39 mL of CH$_3$I (6.3 mmol) and 155 mg (6.4 mmol) of magnesium turnings, and then 11.0 mL of 1.13 M CH$_3$Li in ether (12.4 mmol) was added at −40 °C over 20 min. The mixture was then stirred at −40 °C for a further 1 h. Then a solution of 1-(methoxycarbonyl)adamantane (262 mg, 1.35 mmol) in ether (10 ml) was added at −40 °C over 15 min. After being stirred at room temperature for 1 h, the mixture was quenched with sat. NH$_4$Cl and extracted with ether. The organic layer was washed with 5% NaCl and dried (Na$_2$SO$_4$). The solvent was evaporated, and the residue was purified by flash column chromatography on silica gel (CHCl$_3$) to give **7** (236 mg, 90%) as colorless crystals, mp 70–71 °C. IR (ATR, cm^{-1}), 3478, 2921, 2892, 2849, 1445, 1363, 1142, 929, 887; ^{1}H NMR (500 MHz, C$_6$D$_6$), δ 1.92 (s, 3H), 1.65 (d, *J* 11.6 Hz, 3H), 1.57 (d, *J* 11.6 Hz, 3H), 1.54 (d, *J* 2.4 Hz, 6H), 0.99 (s, 6H), 0.71 (s, 1H, disappeared by D$_2$O treatment); ^{13}C NMR (75.5 MHz, C$_6$D$_6$), δ 73.9, 38.9, 37.4, 36.4, 29.0, 24.5. The observed ^{1}H and ^{13}C NMR spectra agreed with those in the literature.[26,27]

2-(1-Adamantyl)-2-propyl trifluoroacetate (8).[28] Trifluoroacetic anhydride (0.18 mL, 1.3 mmol) was added dropwise to a solution of alcohol **7** (200 mg, 1.03 mmol) and pyridine (4 mL) in CH_2Cl_2 (4 mL), and the reaction mixture was stirred at 0 °C for 2 h. The mixture was washed with cold 10% HCl and cold 5% $NaHCO_3$ and dried (Na_2SO_4). The solvent was evaporated, and the residue was purified by flash column chromatography on silica gel ($CHCl_3$) to give **8** (214 mg, 72%) as a colorless oil. IR (ATR, cm^{-1}), 2908, 1774, 1454, 1373, 1213, 1161, 1123, 1074; ^{1}H NMR (500 MHz, C_6D_6), δ 1.81 (s, 3H), 1.54 (d, *J* 12.2 Hz, 3H), 1.44 (d, *J* 11.6 Hz, 3H), 1.40 (d, *J* 2.4 Hz, 6H), 1.26 (s, 6H); ^{13}C NMR (125 MHz, C_6D_6), δ 156.4 (q, $^2J_{CF}$ 40.3 Hz), 115.4 (q, $^1J_{CF}$ 287.6 Hz), 93.8, 39.8, 36.9, 35.8, 28.6, 19.2. The observed ^{1}H NMR spectrum agreed with that in the literature.[28]

2-(1-Adamantyl)-2-propanethiol (9). Alcohol **7** (29.9 mg, 0.15 mmol) was added to a solution of thiourea (1.75 g, 23 mmol) in a mixture of acetic acid (8 mL) and 47% aqueous HBr (3.8 mL). After being stirred at 25 °C for 6 h, the mixture was poured into cold 15% NaOH (90 mL) and was stirred at room temperature for 16 h. The resultant mixture was cooled to 0 °C and was acidified to pH 2–3 by the addition of 50% H_2SO_4 with the temperature kept below 10 °C. The product was extracted with $CHCl_3$, and the organic layer was washed with 5% $NaHCO_3$ and 5% NaCl and dried (Na_2SO_4). The solvent was evaporated, and the residue was purified by flash column chromatography on silica gel ($CHCl_3$) to give **9** (29 mg, 90%) as pale yellow crystals, mp 119–121 °C. IR (ATR, cm^{-1}), 2900, 2678, 1446, 1361, 1343, 1129; ^{1}H NMR (500 MHz, C_6D_6), δ 1.90 (s, 3H), 1.63 (d, *J* 2.4 Hz, 6H), 1.60 (d, *J* 12.2 Hz, 3H), 1.51 (d, *J* 11.6 Hz, 3H), 1.29 (s, 1H), 1.21 (s, 6H); ^{13}C NMR (125 MHz, C_6D_6), δ 52.1, 38.6, 37.1, 36.7, 29.1, 27.8; HRMS (EI+, *m/z*) for $C_{13}H_{22}S$ (M$^+$): calcd, 210.1442; found, 210.1450.

1-Bromo-3,5,7-tris(1-hydroxy-1-methylethyl)adamantane (4). A solution of CH_3MgI in ether (12 mL) was prepared from 0.38 mL of CH_3I (6.1 mmol) and 152 mg (6.3 mmol) of magnesium turnings, and then 11.0 mL of 1.13 M CH_3Li in ether (12.4 mmol) was added at −40 °C over 30 min. The mixture was then stirred at −40 °C for further 1 h. Then a solution of triester **3** (201 mg, 0.52 mmol) in ether (10 ml) was added at −40 °C over 20 min. After being stirred at room temperature for 1 h, the mixture was quenched with sat. NH_4Cl and extracted with ether. The organic layer was washed with 5% NaCl and dried (Na_2SO_4). The solvent was evaporated, and the residue was purified by flash column chromatography on silica gel ($CHCl_3$) to give **4** (190 mg, 94%) as colorless crystals, mp 200–201 °C (from acetone–$CHCl_3$). IR (ATR, cm^{-1}), 3365, 2969, 1377, 1143, 1121, 948, 910; ^{1}H NMR (300 MHz, acetone-d_6), δ 2.14 (s, 6H), 1.59 (d, *J* 12.3 Hz, 3H), 1.45 (d, *J* 12.1 Hz, 3H), 1.14 (s, 18H), The OH signal was not observed due to rapid proton exchange with water in the solvent; ^{13}C NMR (75.5 MHz, acetone-d_6), δ 73.9, 72.8, 48.6, 45.7, 34.2, 25.2; HRMS (EI+, *m/z*) for $C_{19}H_{27}$ ([M−Br−$3H_2O$]$^+$)[29]: calcd, 255.2113; found, 255.2136.

1-Bromo-3,5,7-tris(1-mercapto-1-methylethyl)adamantane (2). Triol **4** (39.1 mg, 0.10 mmol) was added to a solution of thiourea (3.46 g, 45 mmol) in a mixture of acetic acid (5 mL) and 47% aqueous HBr (2.5 mL). After being stirred at 70 °C for 14 h, the mixture was added to cold 15% NaOH (60 mL) and was stirred at 0 °C for 3 h. The resultant mixture was acidified to pH 2–3 by the addition of 50% H_2SO_4 with the temperature kept below 10 °C, and extracted with $CHCl_3$. The organic layer was washed with 5% $NaHCO_3$ and 5% NaCl and dried (Na_2SO_4). The solvent was then evaporated to give 31.9 mg of a mixture composed of trithiol **2** and partially thiolated products. To achieve complete thiolation, this mixture was treated again using the same amount of thiourea under the same conditions to give 32.0 mg of crude trithiol **2**.

The above procedure was repeated four times, and the combined crude **2** (136 mg) was purified by flash column chromatography on silica gel (AcOEt–$CHCl_3$ 1:3) and subsequently by gel permeation chromatography to give pure **2** (37.6 mg, 21%) as pale yellow crystals, mp 202–204 °C. IR (ATR, cm^{-1}), 2955, 2548, 1461, 1368, 1347, 1122, 1024; ^{1}H NMR (500 MHz, C_6D_6), δ 1.54 (d, *J* 11.6 Hz, 3H), 1.49 (d, *J* 12.2 Hz, 3H), 1.42 (s, 6H), 1.33 (s, 3H), 1.20 (s, 18H); ^{13}C NMR (75.5 MHz, $CDCl_3$), δ 71.4, 52.0, 43.1, 42.9, 34.2, 28.3; HRMS (EI+, *m/z*) for $C_{18}H_{29}S_3$ ([M−Br−CH_4]$^+$)[29]: calcd, 341.1431; found, 341.1402.

Preparation of self-assembled monolayer on gold. Gold substrates with a (111) surface were prepared via vacuum vapor deposition of gold (99.99%) onto freshly cleaved mica sheets (0.05 mm thickness) under high vacuum ($<10^{-3}$ Pa) at a substrate temperature of 580 °C. The deposition was carried out until a 200 nm thickness was obtained. The substrate was annealed at 530 °C for 8 h under air to minimize surface contamination and defects, and was then immersed into 0.1 mM solutions of trithiol **2** at ambient temperature for 15 h or longer. The obtained substrate was washed thoroughly with the same solvent and air-dried.

Cyclic voltammetry. The SAM-modified gold substrate was mounted at the bottom of a cone-shaped cell using an O-ring to serve as a working electrode. The area of the electrode exposed to the electrolyte was 0.152 cm^2 (4.4 mm diameter circle). The reduction wave of thiolate desorption was monitored using 0.5 M aqueous KOH as an electrolyte and a Ag/AgCl reference electrode. The electrolyte solution was deaerated by bubbling argon for 10 min before scanning. Voltammograms were recorded using a BAS ALS600C electrochemical analyzer.

X-ray photoelectron spectroscopy. The XPS data were recorded with a Shimadzu ESCA-3400 spectrometer using a Mg Kα X-ray source (*h*ν 1253.6 eV). The spectra for S 2p and Au 4f were acquired at a pass energy of 75 eV. The photoelectron takeoff angle and the energy resolution were 90° and 0.1 eV, respectively. The binding energies were corrected based on Au 4f$_{7/2}$ at 83.93 eV.[30]

DFT calculations. DFT (density function theory) calculations[31] were performed with the Gaussian 03 program.[32] Optimized structures and their energies were calculated using the UB3LYP method along with the 3-21G basis set for C, H, and S atoms and the LanL2MB basis set for Au. The structures of one Ad(CX$_2$S)$_3$ (X = H or Me) molecule on the finite gold monolayers (Au$_{17}$, Au$_{27}$, or Au$_{37}$) were optimized with symmetric restriction with frozen geometries of finite gold atomic monolayers, where Au–Au distance was fixed at 2.88 Å as a bulk parameter of the Au(111) surface.[1] All stationary points were verified to be either minima (number of imaginary frequency = 0) or transition states by frequency calculations. Single-point calculations of the infinite gold monolayers adsorbed with Ad(CX$_2$S)$_3$ (X = H or Me) molecules were also performed using PBC (periodic boundary conditions) calculations with the optimized geometries of **X1** and **X2** by the UBLYP method at the same basis sets.

Acknowledgements

Supplementary Material

^{1}H and ^{13}C NMR spectra for new compounds and the detailed results of DFT calculations.

References and Notes

1. Poirier, G. E. *Chem. Rev.* **1997**, *97*, 1117–1127.
   https://doi.org/10.1021/cr960074m
2. Love, J. C.; Estroff, L. A.; Kriebel, J. K.; Nuzzo, R. G.; Whitesides, G. M. *Chem. Rev.* **2005**, *105*, 1103–1169.

https://doi.org/10.1021/cr0300789

3. Kind, M.; Wöll, C. *Prog. Surf. Sci.* **2009**, *84*, 230–278.
    https://doi.org/10.1016/j.progsurf.2009.06.001

4. Gooding, J. J.; Mearns, F.; Yang, W.; Liu, J. *Electroanalysis* **2003**, *15*, 81–96.
    https://doi.org/10.1002/elan.200390017

5. Bertin, P. A.; Ahrens, M. J.; Bhavsar, K.; Georganopoulou, D.; Wunder, M.; Blackburn, G. F.; Meade, T. J. *Org. Lett.* **2010**, *12*, 3372–3375.
    https://doi.org/10.1021/ol101180r

6. van Delden, R. A.; ter Wiel, M. K. J.; Pollard, M. M.; Vicario, J.; Koumura. N.; Feringa, B. L. *Nature* **2005**, *437*, 1337–1340.
    https://doi.org/10.1038/nature04127

7. Kay, E. R.; Leigh, D. A.; Zerbetto, F. *Angew. Chem. Int. Ed.* **2007**, *46*, 72–191.
    https://doi.org/10.1002/anie.200504313

8. Tour, J. M. *Acc. Chem. Res.* **2000**, *33*, 791–804.
    https://doi.org/10.1021/ar0000612

9. McCreery, R. L. *Chem. Mater.* **2004**, *16*, 4477–4496.
    https://doi.org/10.1021/cm049517q

10. Kitagawa, T.; Idomoto, Y.; Matsubara, H.; Hobara, D.; Kakiuchi, T.; Okazaki, T.; Komatsu, K. *J. Org. Chem.* **2006**, *71*, 1362–1369.
    https://doi.org/10.1021/jo051863j

11. Kitagawa, T.; Matsubara, H.; Komatsu, K.; Hirai, K.; Okazaki, T.; Hase, T. *Langmuir* **2013**, *29*, 4275–4282.
    https://doi.org/10.1021/la305092g

12. Kitagawa, T.; Matsubara, H.; Okazaki, T.; Komatsu, K. *Molecules* **2014**, *19*, 15298–15313.
    https://doi.org/10.3390/molecules190915298

13. Hatano, M.; Matsumura, T.; Ishihara, K. *Org. Lett.* **2005**, *7*, 573–576.
    https://doi.org/10.1021/ol047685i

14. Bandgar, B. P.; Sadavarte, V. S.; Uppalla, L. S. *Chem. Lett.* **2000**, *29*, 1304–1305.
    https://doi.org/10.1246/cl.2000.1304

15. Tkachenko, B. A.; Fokina, N. A.; Chernish, L. V.; Dahl, J. E. P.; Liu, S.; Carlson, R. M. K.; Fokin, A. A.; Schreiner, P. R. *Org. Lett.* **2006**, *8*, 1767–1770.
    https://doi.org/10.1021/ol053136g

16. Castner, D. G.; Hinds, K.; Grainger, D. W. *Langmuir* **1996**, *12*, 5083–5086.
    https://doi.org/10.1021/la960465w

17. Ishida, T.; Choi, N.; Mizutani, W.; Tokumoto, H.; Kojima, I.; Azehara, H.; Hokari, H.; Akiba, U.; Fujihira, M. *Langmuir* **1999**, *15*, 6799–6806.
    https://doi.org/10.1021/la9810307

18. Bensebaa, F.; Zhou, Y.; Deslandes, Y.; Kruus, E.; Ellis, T. H. *Surf. Sci.* **1998**, *405*, L472–L476.
    https://doi.org/10.1016/S0039-6028(98)00097-1

19. Imabayashi, S.; Iida, M.; Hobara, D.; Feng, Z. Q.; Niki, K.; Kakiuchi, T. *J. Electroanal. Chem.* **1997**, *428*, 33–38.
    https://doi.org/10.1016/S0022-0728(97)00006-5

20. Kakiuchi, T.; Usui, H.; Hobara, D.; Yamamoto, M. *Langmuir* **2002**, *18*, 5231–5238.
    https://doi.org/10.1021/la011560u

21. This charge value is 37% greater than the theoretical value, 73 μC/cm^2, which is expected based on a ($\sqrt{3}$ × $\sqrt{3}$)R30° packing pattern for adsorbed sulfur atoms. This difference is due to the surface roughness of the

Au substrate and to a discharge current that results from the removal of the adsorbed molecules upon reduction.[20]

22. Molina, L. M.; Hammer, B. *Chem. Phys. Lett.* **2002**, *360*, 264–271.
https://doi.org/10.1016/S0009-2614(02)00841-2

23. Batsanov, S. S. *Inorg. Mater.* **2001**, *37*, 871–885.
https://doi.org/10.1023/A:1011625728803

24. Malgrange, C.; Ricolleau, C.; Schenker, M. *Symmetry and Physical Properties of Crystals*; Springer: Dordrecht, **2014**, Chapter 3.
https://doi.org/10.1007/978-94-017-8993-6

25. Oura, K.; Lifshits, V. G.; Saranin, A. A.; Zotov, A. V.; Katayama, M. *Surface Science: An Introduction*, Springer: Berlin, **2003**, Chapter 2.
https://doi.org/10.1007/978-3-662-05179-5

26. Yurchenko, A. G.; Fedorenko, T. V. *Zh. Org. Khim.* **1987**, *23*, 970–976.

27. Fuchs, W.; Kalbacher, H.; Voelter, W., *Org. Magn. Reson.* **1981**, *17*, 157–162.
https://doi.org/10.1002/mrc.1270170302

28. Mutulis, F.; Polis, J.; Raguele, B.; Sekacis, I.; Mishnev, A. F.; Cipens, G. *Zh. Org. Khim.* **1989**, *25*, 558–565.
https://doi.org/10.1021/jp010127q

29. Excessive fragmentation occurred even with a low electron beam energy of 20 eV.

30. Heister, K.; Zharnikov, M.; Grunze, M.; Johansson, L. S. O. *J. Phys. Chem. B* **2001**, *105*, 4058–4061.

31. Koch, W.; Holthausen, M. C. *A Chemist's Guide to Density Functional Theory*; 2nd ed., Wiley-VCH, Weinheim, **2000**.

32. Frisch, M. J.; Trucks, G. W.; Schlegel, H. B.; Scuseria, G. E.; Robb, M. A.; Cheeseman, J. R.; Montgomery, J. A., Jr.; Vreven, T.; Kudin, K. N.; Burant, J. C.; Millam, J. M.; Iyengar, S. S.; Tomasi, J.; Barone, V.; Mennucci, B.; Cossi, M.; Scalmani, G.; Rega, N.; Petersson, G. A.; Nakatsuji, H.; Hada, M.; Ehara, M.; Toyota, K.; Fukuda, R.; Hasegawa, J.; Ishida, M.; Nakajima, T.; Honda, Y.; Kitao, O.; Nakai, H.; Klene, M.; Li, X.; Knox, J. E.; Hratchian, H. P.; Cross, J. B.; Bakken, V.; Adamo, C.; Jaramillo, J.; Gomperts, R.; Stratmann, R. E.; Yazyev, O.; Austin, A. J.; Cammi, R.; Pomelli, C.; Ochterski, J. W.; Ayala, P. Y.; Morokuma, K.; Voth, G. A.; Salvador, P.; Dannenberg, J. J.; Zakrzewski, V. G.; Dapprich, S.; Daniels, A. D.; Strain, M. C.; Farkas, O.; Malick, D. K.; Rabuck, A. D.; Raghavachari, K.; Foresman, J. B.; Ortiz, J. V.; Cui, Q.; Baboul, A. G.; Clifford, S.; Cioslowski, J.; Stefanov, B. B.; Liu, G.; Liashenko, A.; Piskorz, P.; Komaromi, I.; Martin, R. L.; Fox, D. J.; Keith, T.; Al-Laham, M. A.; Peng, C. Y.; Nanayakkara, A.; Challacombe, M.; Gill, P. M. W.; Johnson, B.; Chen, W.; Wong, M. W.; Gonzalez, C.; Pople, J. A. Gaussian 03, Revision E.01, Gaussian, Inc., Wallingford CT, **2004**.